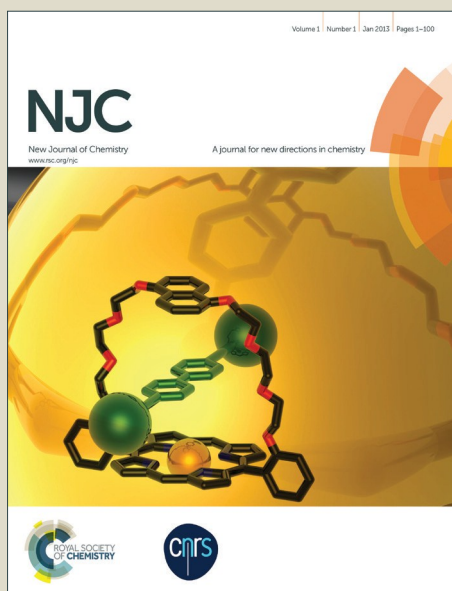


NJC

Accepted Manuscript



This article can be cited before page numbers have been issued, to do this please use: S. Khattab, S. E. Abdel Naim, M. El-Sayed, A. A. El Bardan, A. O. Elzoghby, A. A. Bekhit and A. El-Faham, *New J. Chem.*, 2016, DOI: 10.1039/C6NJ02539K.



This is an *Accepted Manuscript*, which has been through the Royal Society of Chemistry peer review process and has been accepted for publication.

Accepted Manuscripts are published online shortly after acceptance, before technical editing, formatting and proof reading. Using this free service, authors can make their results available to the community, in citable form, before we publish the edited article. We will replace this *Accepted Manuscript* with the edited and formatted *Advance Article* as soon as it is available.

You can find more information about *Accepted Manuscripts* in the [Information for Authors](#).

Please note that technical editing may introduce minor changes to the text and/or graphics, which may alter content. The journal's standard [Terms & Conditions](#) and the [Ethical guidelines](#) still apply. In no event shall the Royal Society of Chemistry be held responsible for any errors or omissions in this *Accepted Manuscript* or any consequences arising from the use of any information it contains.



New Journal of Chemistry

Full paper

Design and Synthesis of New s-Triazine Polymers and its Application as Nanoparticulate Drug Delivery Systems

Sherine N. Khattab,^{a,*} Samar E. Abdel Naim,^a Mousa El-Sayed,^a Aly A. El Bardan,^a Ahmed O. Elzoghby,^{b,c} Adnan A. Bekhit^d and Ayman El-Faham^{a,e*}

Received 00th January 20xx,
Accepted 00th January 20xx

DOI: 10.1039/x0xx00000x

www.rsc.org/

Herein, we report the synthesis of a library of new s-triazine polyamides containing glycine and thioglycolic acid. The reaction of s-triazine dicarboxylic acid derivatives with ethylenediamine, benzidine, piperazine or p-phenylenediamine, afforded the target designed s-triazine polyamides. Thermal properties of the polymers were evaluated by different techniques. Thermodynamic parameters of decomposition processes were evaluated. The feasibility of the synthesized polymers as drug nano-delivery systems was investigated. The nanoparticles were loaded with celecoxib (CXB), an anti-inflammatory drug with a highly promising anti-cancer effect, resulting in high entrapment efficiency levels (62.3–99.8%) with a good drug loading in the range of 1.58–4.19%. After 48 h, 46.90, 64.20, 57.81, 53.95, and 49.43% of CXB was released from polymeric NPs **26**, **43**, **44**, **45** and **46**, respectively, demonstrating a sustained drug release profile. Notably, free CXB, and CXB-loaded polymeric NPs **CXB-43**, **CXB-45**, and **CXB-46** demonstrated considerable reduction in cell viability in a dose-dependent manner.

Introduction

The design of suitable polymeric materials is an increasingly important research area due to demands for applications as biomedical, pharmaceutical, artificial surgical implants and scaffolds for tissue engineering.^{1–4} Many efforts have been recently dedicated to design, investigate and synthesize biocompatible, biodegradable polymers for medicinal applications in either the fabrication of biodegradable devices or as drug delivery systems.^{2,5–8}

Natural polymers suffer from some disadvantages such as microbial contamination, batch to batch variation dependent on environmental and seasonal factors,⁹ uncontrolled rate of hydration which result in variation in the percentage of chemical constituents, due to differences in the collection of natural materials at different times as well as differences in region, species, and climate conditions, and reduced viscosity on storage.¹⁰ The use of synthetic polymer overcomes above disadvantages and hence their use in

formulation is preferred.

The most important advantages of biodegradable polymers as drug carriers include: localized delivery of the drug to the target site of action, sustained drug release, and stabilization of the unstable drugs.¹¹

Aliphatic polyesters are the most explored family of biodegradable polymers. Although numerous variations of aliphatic polyesters based on L-lactic acid, glycolic acid, ε-caprolactone, and their copolymers have been used as biodegradable biomaterials,^{12,13} they still lack certain optimum properties.^{14,15} For example, polymer degradation rate depends on many factors, such as molecular structure and composition of the polymer, molecular weight of the polymer, polymer crystallinity, percent of the cross-linking present in the polymeric chain, and additives, etc.¹⁶ The hydrolytic degradation of poly(α-hydroxyacids) is mostly influenced by four major factors: (1) the hydrolysis rate constant of the ester bond; (2) the diffusion coefficient of water in the polymer matrix; (3) the diffusion coefficient of the chain fragments within the polymeric matrix and (4) the solubility of the degradation product.^{15, 17} In addition, it has been reported that the acidic degradation by-products of these polyesters are toxic to some cells, limiting their use as functional tissue engineering scaffolds.^{18,19} In attempt to address these limitations, poly (α-amino acids) and polyamides containing α-amino acids have been considered.^{5,20,21} Among the synthetic polyamides, only those containing the naturally occurring α-amino acids, being structurally close to the natural polypeptides, have potentially degradable linkages which make them suitable as biomaterials.^{6,7,22–24} In the aim to create polymers containing naturally occurring α-amino acids various approaches have been carried out successfully in the synthesis of new type of monomers.

^a Department of Chemistry, Faculty of Science, Alexandria University, P.O. Box 426, Ibrahimia, Alexandria 21321, Egypt. E-mail: sh.n.khattab@gmail.com

^b Department of Industrial Pharmacy, Faculty of Pharmacy, Alexandria University, Alexandria 21521, Egypt.

^c Cancer Nanotechnology Research Laboratory (CNRL), Faculty of Pharmacy, Alexandria University, Alexandria 21521, Egypt.

^d Department of Pharmaceutical Chemistry, Faculty of Pharmacy, Alexandria University, Alexandria 21521, Egypt.

^e Department of Chemistry, College of Science, King Saud University, P.O. Box 2455, Riyadh 11451, Saudi Arabia. E-mail: aymanel_faham@hotmail.com

† Footnotes relating to the title and/or authors should appear here.

Electronic Supplementary Information (ESI) available: [details of any supplementary information available should be included here]. See DOI: 10.1039/x0xx00000x

Besides the large number of vinylic monomers containing α -amino acids as pendants, monomers suitable for polycondensation, polyaddition or ring-opening polymerization also were obtained from these metabolites. Diamine type monomers derived from glycine (Gly),^{25,26} (D,L)- and (L)-alanine (Ala),^{27–29} (D,L)- and (L)-phenylalanine (Phe),³⁰ and various aliphatic diols or from tyrosine-leucine-dipeptide (Tyr–Leu)²⁶ and different diamines, were utilized in the obtainment of polyester amides (PEAs) or polyamides. Preliminary biodegradation studies demonstrated that these polymers degrade both hydrolytically and enzymatically.³¹ Furthermore, polyamides (PAs) derived from C₁₀ and C₁₄ dicarboxylic acids and diamines derived from 1,6-hexanediamine or 1,12-dodecanediamine and L-phenylalanine, L-valyl-L-phenylalanine or L-phenylalanyl-L-valine residues have been reported as biocompatible polymers.^{32,33} Moreover, the presence of the amide group provides a focal point for hydrogen bonding, which results in the formation of crystalline structures that are characterized by toughness, resistance to oils and solvents, superior physical strength, a degree of sensitivity to moisture and high melting points. Because of these versatile properties and applications, many research activities have been undertaken to synthesize new polyamides and to modify them for desired properties.³⁴ Since early 2000's, polyamide polymers^{35,36} have been investigated in cancer nanomedicines. Polymeric nanocarriers provide the possibility to encapsulate water insoluble drug, protect unstable bioactives, and modify their pharmacokinetics and systemic circulation behavior. These properties are interesting in the field of oncology by encapsulating anti-cancer drugs within nanoparticles to reduce their toxicity and improve their physicochemical properties.^{37,38} Biodegradable polymers including polyamides and polyesters are commonly utilized for development of nanoparticles as delivery systems for anti-cancer drugs. The enhanced permeability and retention (EPR) effect has been considered the gold standard in anti-cancer drug delivery. It describes the process by which polymeric nanocarriers can be delivered to the tumor interstitium where leaky tumor vessels allow macromolecular extravasation into the tumor tissue through the capillaries fenestrations.³⁹ These endothelial fenestrations can reach sizes ranging from 200 to 2000 nm, depending on the tumor type, its surrounding environment and its region.^{38,39} However, nanoparticles may undergo rapid clearance from the circulation following their opsonization and uptake by the reticuloendothelial (RES) system. Since opsonization process occurs mainly via hydrophobic interactions between the carrier surface and opsonins, modification of nanoparticle surface with hydrophilic polymers (e.g. PEG or poloxamer) can be utilized for development of long-circulating nanocarriers.⁴⁰ Thus, the aim of this study was extrapolated to the design of therapeutic nanoparticles based on the synthesized polymers for treatment of cancer. Therefore, our trial is to prepare small sized drug-loaded polymeric nanoparticles with hydrophilic poloxamer coat allowing their prolonged circulation and enabling extravasation through tumor fenestrations and subsequent accumulation in tumor tissue by the EPR effect.

The synthesis of triazine polymers have been considerably investigated by different research groups.^{34,41} The properties of the *s*-triazine polymers are influenced by the nature of substituents on the *s*-triazine nucleus and also by the nature of diamine components of polymer chain. These aromatic polyamides are promising materials of high thermal stability and processibility. Sojitra *et al.*⁴¹ synthesized a new set of high-performance polyamides based on *s*-triazine ring as flexibilizing linkages into the backbone of wholly aromatic polyamides which results in soluble polyamides with higher thermal stability along with good processibility.

We have previously described the synthesis and thermal properties of new type of polyamides-containing amino acids based on new symmetric meta-oriented protected diamines derived from coupling of amino acids with *m*-phenylenediamine or 2,6-diaminopyridine.⁴² A family of polyamides based on benzene dicarboxylic acid, pyridine dicarboxylic acid, and α -amino acid linked to benzidine and 4,4'-oxydianiline was also recently studied.⁴³ Here we describe another family of polyamides based on triazine moiety containing glycine and thioglycolic acid with diamines, such as ethylenediamine, benzidine, piperazine and *p*-phenylenediamine, to study the effect of triazine moiety incorporated with glycine and thioglycolic acid on the nature and thermal stability of the polymers. The incorporation of morpholine, piperidine and aniline to the triazine moiety was also studied in attempt to increase the hydrophobicity of the target polyamides.

Results and Discussion

Chemistry

Preparation of *s*-triazine polyamides containing glycine and thioglycolic acid.

Preparation of *s*-triazine dicarboxylic acid derivatives 9-14:

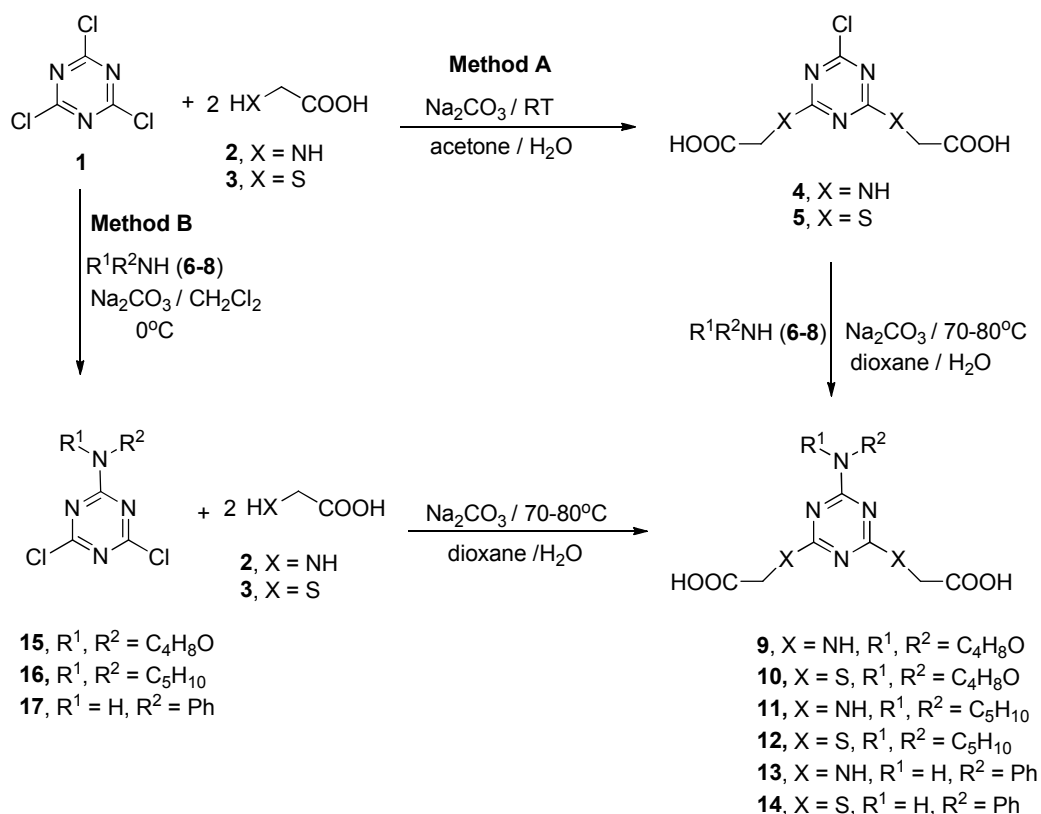
The *s*-triazine dicarboxylic acid derivatives **9-14** were prepared by two methods. In method A, the two chloride atoms of cyanuric chloride were replaced by two glycine or two thioglycolic acid molecules, while the third chloride was replaced with piperidine, morpholine, or aniline group respectively. 2,2'-(6-morpholino/piperidino/phenylamino-1,3,5-triazine-2,4-diyl)bis(azanediy/sulfanediy)diacetic acid derivatives **9-14** were prepared through the following sequential reaction: cyanuric chloride **1** was reacted first with two equivalent glycine or two thioglycolic acid in the presence of sodium carbonate (acid scavenger) to afford the corresponding products, 2-chloro-4,6-disubstituted-1,3,5-triazine derivatives **4** and **5**, respectively. Compounds **4** or **5** were allowed to react with piperidine, morpholine or aniline at 70–80°C in the presence of sodium carbonate in dioxane as solvent as shown in Scheme 1. Compounds **9-14** were also prepared by the replacement of one chloride atom of cyanuric chloride with piperidine, morpholine, or aniline group at 0°C, followed by subsequent replacement of the two chloride atoms with two equivalent glycine or two thioglycolic acid molecules at

70–80°C in the presence of sodium carbonate in dioxane as solvent, (Scheme 1, method B).

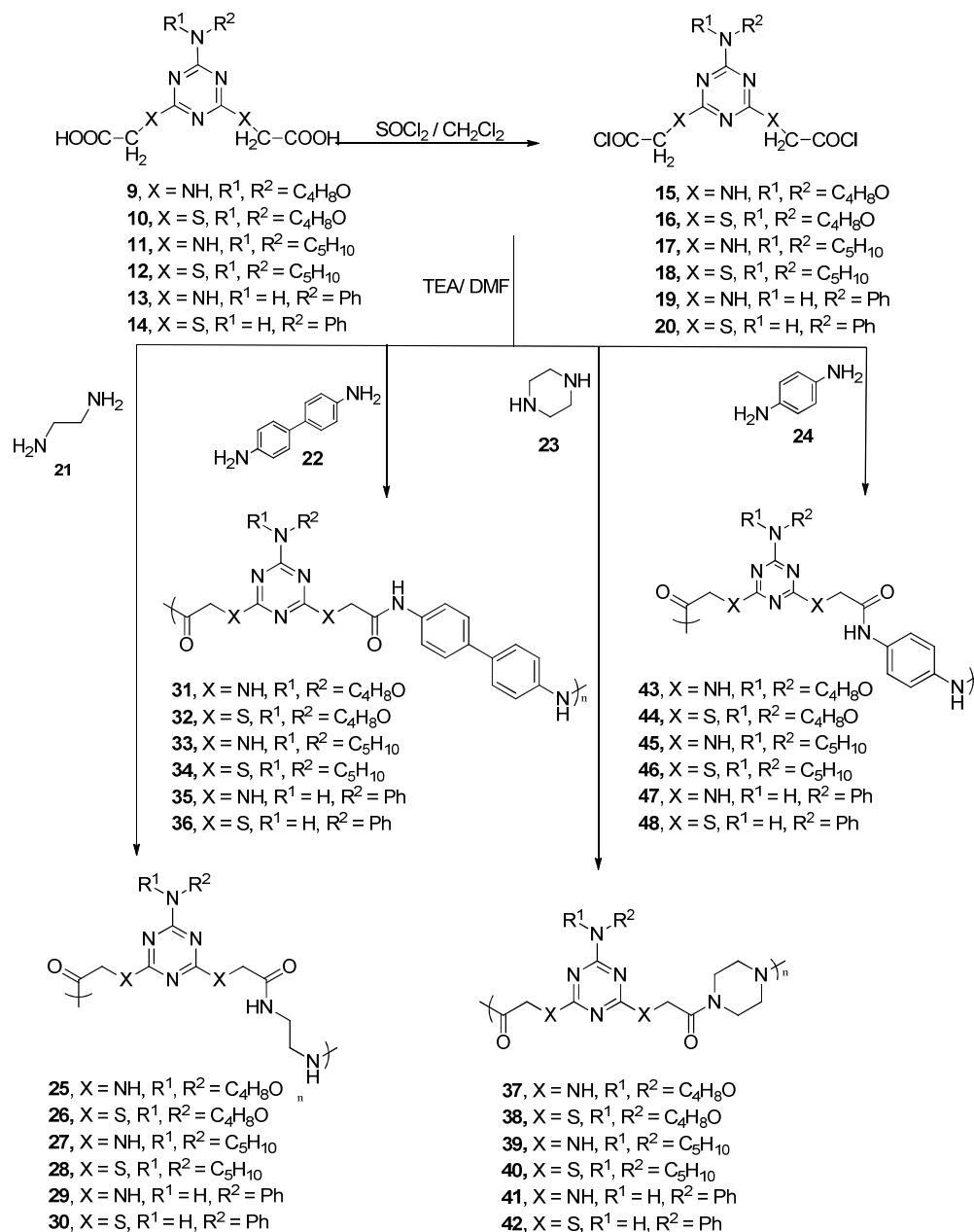
Preparation of *s*-triazine polyamides 25–48. The *s*-triazine dicarboxylic acid chloride derivatives **15–20** used in this investigation were prepared by the reaction of their corresponding dicarboxylic acids, with thionyl chloride and dichloromethane as solvent. Direct polycondensation reaction of an equimolar mixture of the acid chloride derivatives **15–20** with the diamines (ethylenediamine **21**, benzidine **22**, piperazine **23** or *p*-phenylenediamine **24**), in presence of triethyl amine (TEA) as base, in DMF solution at 0–5°C furnished the corresponding *s*-triazine polyamides **25–48**, respectively in high yields, Scheme 2. The polymer structures were confirmed by elemental analysis, IR spectroscopy.

Physical Properties of the Prepared Polyamides Containing Amino Acids

Solubility: The prepared *s*-triazine polyamides **25–48** showed similar solubility behavior in different organic solvents. Moderate to complete dissolution was observed in a variety of aprotic solvents such as NMP, DMSO, DMAc, boiling alcoholic solvents such as methanol, ethanol while insoluble in halogenated solvents such as CHCl₃, CCl₄, CH₂Cl₂, ClCH₂CH₂Cl or in ethers such as Et₂O, THF, 1,4-dioxane or 1,2-dimethoxyethane (DME).



Scheme 1: Synthesis of triazine dicarboxylic acid monomers 9–14



Scheme 2: Synthesis of polyamides 25-48

FT IR Spectroscopy: The FT IR spectra of the polymers exhibited characteristic absorbance at the range of ν 3445-3348 cm^{-1} and 1698-1601 cm^{-1} , corresponding to the N-H and C=O stretching of the amide group, respectively. Bands around ν 2800-2900 cm^{-1} were assigned to the alkyl H-C stretching.

Thermal Properties: The thermal properties of the prepared polymers were evaluated by thermogravimetric analysis (TGA), derivatives thermogravimetry (DTG), differential thermal analysis (DTA), and differential scanning calorimetry (DSC) techniques. Thermogravimetry (TG) is a technique in which the weight of a sample is measured as a function of temperature whilst it is subject to a controlled heating program. Derivatives thermogravimetry

(DTG) is a method of expressing the results of TG by giving the first derivative curve as a function of temperature or time to precisely locate the temperature transitions. Differential thermal analysis (DTA) detects the change in the heat content (enthalpy) with changing temperature. DSC measures the temperatures and heat flows associated with transitions in materials as a function of time and temperature in a controlled atmosphere. A controlled thermal program is operative. The thermal properties of these new materials were carried out in the temperature range from 20 °C to 700 °C in air atmosphere. Samples were heated at a heating rate of 10°C/min.

Figure 1 shows as a prototype, the TGA/DTG curves of the glycine-containing polymers **25**, **27**, **29** and thioglycolic acid-containing polymers **26**, **28**, **30**, derived from the ethylene diamine **21**, respectively. Structure-thermal property correlation based on changing the diacid residue and the amine substituent at the triazine moiety, revealed that the prepared polymers have comparable thermal stabilities.

Glycine-containing polymers **25**, **27**, **29** exhibited subsequent major degradation processes and their major amide linkage degradation processes appeared at 568°C (82.2 % wt loss), 555°C (89.7 % wt loss) and 557°C (87.4 % wt loss) leaving 17.8 %, 10.3 % and 12.6 %, respectively, as remaining mass residues (Table S1, SI). Thioglycolic acid-containing polymers **26**, **28**, **30** exhibited also subsequent major degradation and their major amide linkage degradation processes appeared at 568°C (84.4 % wt loss), 560°C (94.5 % wt loss) and 544°C (74.4 % wt loss) leaving 15.6 %, 5.5 % and 25.6 %, respectively, as remaining mass residues (Table S1, SI).

On the other hand, glycine-containing polymers **31**, **33** and **35**, derived from the diamine, benzidine **22**, exhibited their major amide linkage degradation processes at 542°C (99.7 % wt loss), 508°C (96.6 % wt loss) and 516°C (90.2 % wt loss) leaving 0.3 %, 3.4 % and 9.8 %, respectively, as remaining mass residues (Table S1, SI). Thioglycolic acid-containing polymers **32**, **34**, **36**, derived from the diamine, benzidine **22**, exhibited also subsequent major degradation and their major amide linkage degradation processes appeared at 563°C (92.8 % wt loss), 582°C (99.0 % wt loss) and 498°C (89.5 % wt loss) leaving 7.2 %, 1.0 % and 10.5 %, respectively, as remaining mass residues (Table S1, SI).

Glycine-containing polymers **37**, **39**, **41** and **43**, **45**, **47** and thioglycolic acid-containing polymers **38**, **40**, **42** and **44**, **46**, **48** derived from the diamine, piperazine **23** and *p*-phenylenediamine **24** respectively, gave similar thermal properties to the previous discussed polymer series. These results revealed the thermal stability of the newly synthesized polyamides.

The thermodynamic parameters of decomposition processes of polymers, namely, activation energy ΔE_a , enthalpy (ΔH), entropy (ΔS) were evaluated by employing the Horowitz–Metzger equation,⁴⁴ (Table S2, SI). The order of chemical reactions (n) was calculated via the peak symmetry method by Kissinger.⁴⁵ The asymmetry of the peak, S , was calculated as follows:

$$S = 0 : 63n^2$$

$$n = 1.26 (a/b)^{1/2}$$

The value of the decomposed substance fraction, α_m , at the moment of maximum development of reaction (with $T = T_m$) was determined from the relation.⁴⁶

$$(1 - \alpha_m) = n^{1/1-n}$$

The values of collision factor, Z , can be obtained by making the use of the relation.⁴⁷

$$Z = (E_a^* / RT_m) \beta \exp(E_a^* / RT_m^2)$$

where R is the molar gas constant, β is the heating rate ($K S^{-1}$), T_m is the peak temperature.

The entropies of activation ΔS are calculated from the equation:⁴⁸

$$Z = (kT_m/h) \exp \Delta S / R$$

where k is Boltzmann constant and h is Planck's constant.

The change in enthalpy (ΔH^*), taking place at any peak temperature, T_m , can be given by the following equation:

$$(\Delta S^*) = \Delta H^* / T_m$$

Based on least square calculations, the $\ln \Delta t$ versus $1000/T$ plots for all polymers, for each DTA curve, gave straight lines from which the activation energies were calculated according to the method of Piloyan et al.⁴⁹ The slopes were of the Arrhenius type and equals to $\Delta E_a^* / R$.

According to the kinetic data obtained from DTA curves all polymers have negative entropy (ΔS^*), which are nearly of the same magnitude (-0.231 to -0.249) $KJ mol^{-1}$, which indicates ordered systems and more ordered activated states that may be possible through the chemisorption of other light decomposition products. Indicating that the transition states are more ordered than the reactants, thus in a less random molecular configuration than the Reactants.⁵⁰ The kinetic data obtained from the nonisothermal decomposition of the prepared polymers are given in Table S2; Supporting Information.

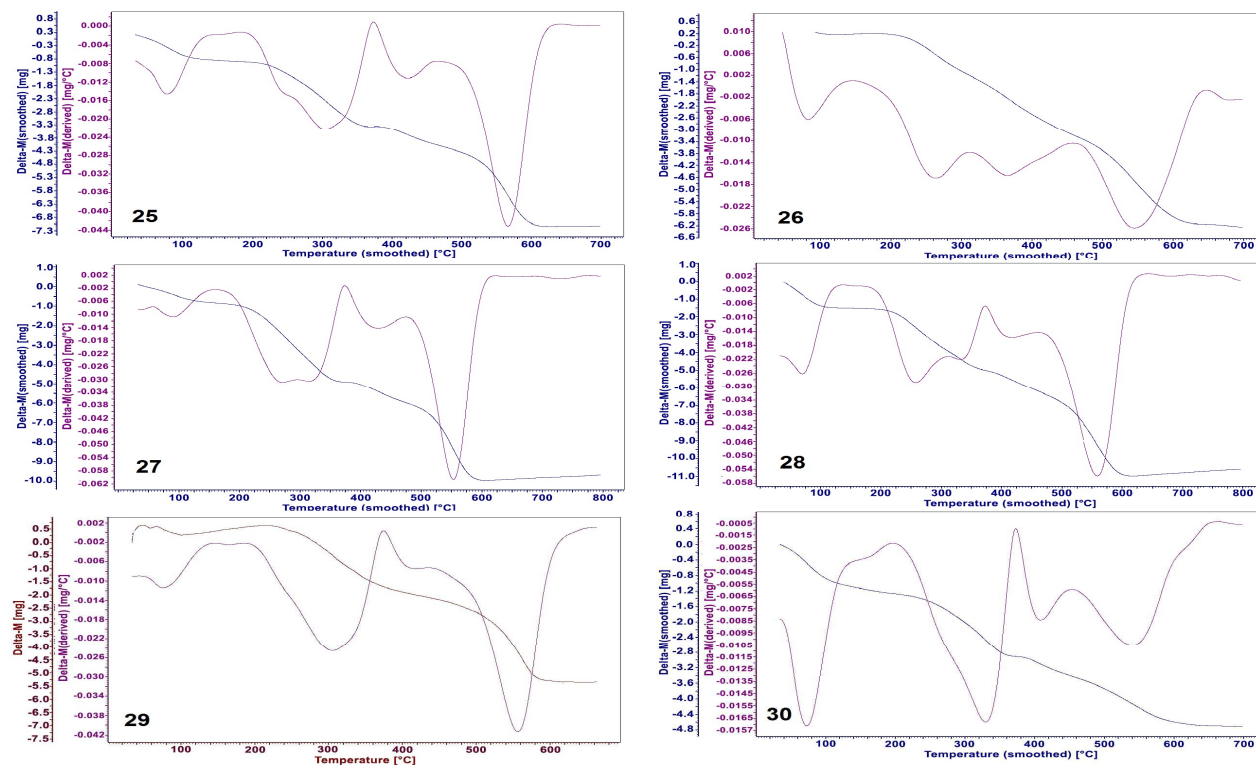


Figure 1: TGA/DTG curves of glycine-containing polymers **25**, **27**, **29** and thioglycolic acid-containing polymers **26**, **28**, **30**.

All the polymers possess high activation energy values assigning their high stability. It is observed that many polyamides have nearly the same E_a values for the all decomposition steps, indicating a similar degradation mechanism in these compounds. For instance, polymers (**26**, **29**, **42**) and (**28**, **35**, **38**, **47**) and (**27**, **33**, **34**, **39**, **44**, **46**, **48**) have the same E_a at the last decomposition step, (Table S2, SI).

Thermal transitions of polyamides **25-48** observed from DSC curves, indicate that most polymers exhibited a melting and glass transition peak indicating that most of the polymers are amorphous. The glass transition temperature (T_g) of the newly synthesized polymers ranged from 280°C to 452°C. The melting temperature, T_m , of all polymers ranged from 505°C to 643°C, indicating the high stability of the polymers.

In general, it is to be expected that derivatives of glycine could be highly crystalline with extensive hydrogen bonding in contrast to the amorphous character of polymers that could be synthesized from α -amino acids with bulky side groups.

Biology

Drug-loaded polymeric nanoparticles. In this study, drug-loaded nanoparticles were successfully fabricated from the synthesized polymers via nanoprecipitation/solvent displacement technique.⁵¹ This technique involves spontaneous precipitation of the hydrophobic polymer into nanoparticles with the adsorption of pluronic (poloxamer) molecules onto their surface when an organic solution of polymer and drug was introduced into aqueous solution containing the poloxamer stabilizer.⁵² In pharmaceutical industry, pluronics[®] have been used as emulsifiers, solubilizers, surfactant stabilizers, and wetting agents.

Pluronic[®] (poloxamers) are nonionic amphiphilic triblock polymers composed of PEO–PPO–PEO alternating units with the general formula $\text{HO}(\text{C}_2\text{H}_4\text{O})_a(\text{C}_3\text{H}_6\text{O})_b(\text{C}_2\text{H}_4\text{O})_a\text{H}$. PEO/PPO block copolymers can be adsorbed onto surface of hydrophobic nanoparticulate systems via their hydrophobic PPO central block whereas the hydrophilic PEO chains protrudes to the external aqueous medium providing steric stabilization to the nanoparticles.^{53,54}

By the centrifugation-washing step, the excess molecules of unadsorbed pluronic® could be eliminated from the bulk. All nanoparticle samples were easily redispersible in water and showed enhanced wettability by virtue of the surface presence of PEO residues of pluronic providing hydrophilicity to the nanoparticle surface.

Celecoxib (CXB) is an anti-inflammatory NSAID that specifically inhibits COX-2 and has drawn much attention for its anti-cancer properties. The COX-2 inhibitor reduces mammary tumor incidence induced by (7, 12-dimethylbenz[a]anthracene) DMBA in rats. It is also effective in blocking the growth of breast cancer xenografts in nude mice. CXB could evoke cell cycle arrest, anti-angiogenesis, and apoptotic cell death in cancers. It has also been used for treatment of lung cancer, colorectal cancer, colon cancer, ultraviolet (UV) light-induced skin cancer and breast cancer.^{55,56}

The method of nanoparticle preparation is highly desirable for hydrophobic compounds, such as celecoxib (CXB) resulting in high entrapment efficiency levels (62.3% to 99.8%) with a good drug loading in the range of 1.58%–4.19% (Table 1), a favorable parameter for increasing efficacy of targeted drug delivery. Dynamic light scattering (DLS) measurements of the particle size of CXB-loaded polymeric NPs are presented in Table 1. The size of NPs ranged from 176.4 to 265.2 nm.

Table 1: Physicochemical properties of CXB-loaded polymeric NPs.

Polymer	Entrapment Efficiency, EE (% w/w)	Drug Loading, DL (% w/w)	Particle size (nm)	PDI	Zeta potential (mV)
CXB-26	71.3	1.58	209.1	0.219	-31.2
CXB-43	68.2	3.25	183.9	0.257	-24.2
CXB-44	98.3	2.32	245.7	0.258	-37.9
CXB-45	62.3	2.97	176.4	0.280	-32.9
CXB-46	99.8	4.19	265.2	0.304	-27.0

As a prototype, **Figure 2a** shows a representative particle size distribution of CXB-loaded polymeric NPs of **CXB-46**. A unimodal particle size distribution was observed where the particles have a size of 265.2 nm with polydispersity of 0.304-0.338. Such small size of the prepared nanoparticles leads to a reduction in the rate of clearance by the RES and thus an extended plasma circulation

time.³⁸ Therefore, we can predict our NPs, by virtue of their size and hydrophilic poloxamer corona, to have prolonged circulating behavior in systemic circulation thus enabling accumulation in tumor tissue by the EPR effect. Zeta potential measurements of the CXB-loaded polymeric NPs are presented in Table 1. The NPs were negatively charged with a zeta potential of -24.2 to -37.9 mV (**Figure 2b**) indicating a good colloidal stability against aggregation.

TEM micrographs of the CXB-loaded polymeric NPs **CXB-46** showed small monodispersed spherical NPs with a core-shell structure (**Figure 3**). This may be explained by the hydrophilic shell of pluronic layer adsorbed onto the surface of the hydrophobic polymer nanoparticle core. The aggregation of NPs was prevented effectively via the stabilizing effect of pluronic which provide a surface layer surrounding the NPs and stabilizes it through steric repulsion.⁵² The diameter of NPs was smaller than that obtained from DLS measurements. The DLS method gives the hydrodynamic diameter, and the nanoparticles may shrink during the sample drying and preparation for TEM.³⁶

The FTIR spectra of the CXB-loaded polymeric NPs, **CXB-26**, **CXB-43**, **CXB-44**, **CXB-45**, **CXB-46**, exhibited two characteristic absorbance peaks at the range of ν 3397-3282 cm^{-1} corresponding to the symmetric and asymmetric stretching of NH_2 group of **CXB**. Moreover, two bands at the range of ν 1378-1084 cm^{-1} were assigned to the symmetric and asymmetric stretching of the drug SO_2 group. Thus, the FT IR spectra of CXB-loaded polymeric NPs indicate the successful entrapment of the drug within the nanoparticles. The in vitro cumulative release profiles of CXB from different polymeric NPs are shown in (**Figure 4**). It was found that after 48 h, 46.9%, 64.20%, 57.81%, 53.95%, and 49.43% of CXB was released from polymeric NPs **CXB-26**, **CXB-43**, **CXB-44**, **CXB-45** and **CXB-46** respectively. This result showed that the nanocarrier cannot only solubilize the poorly soluble drug, **CXB**, but also sustain its release. A sustained-release pattern is a key issue in the development of colloidal drug delivery systems used in the field of nanomedicine. Drugs must be released slowly from polymeric NPs because fast release of drugs from NPs causes precipitation of the hydrophobic drug in the systemic circulation.⁵⁷

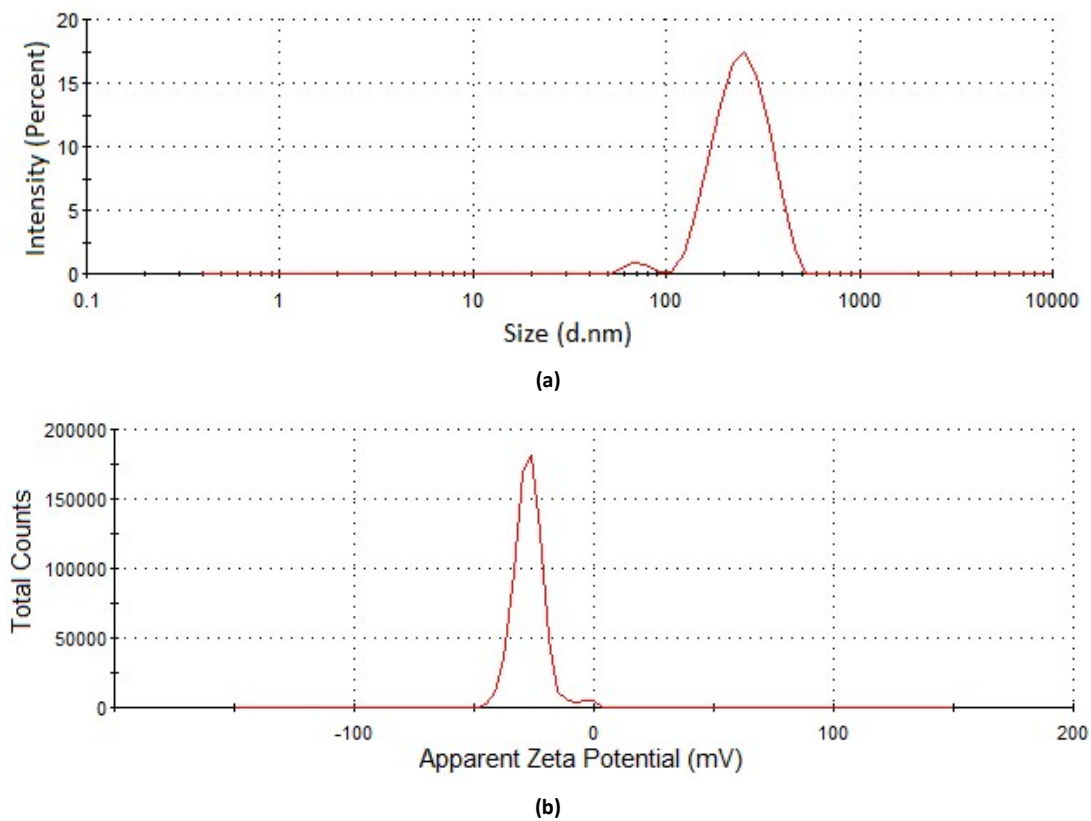


Figure 2: Particle size (a) and zeta potential (b) distribution of CXB-loaded polymeric NPs (CXB-46).

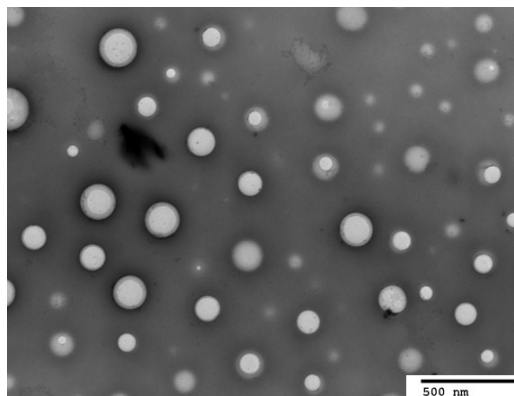


Figure 3: Transmission electron micrograph (TEM) of CXB-loaded polymeric NPs CXB-46.

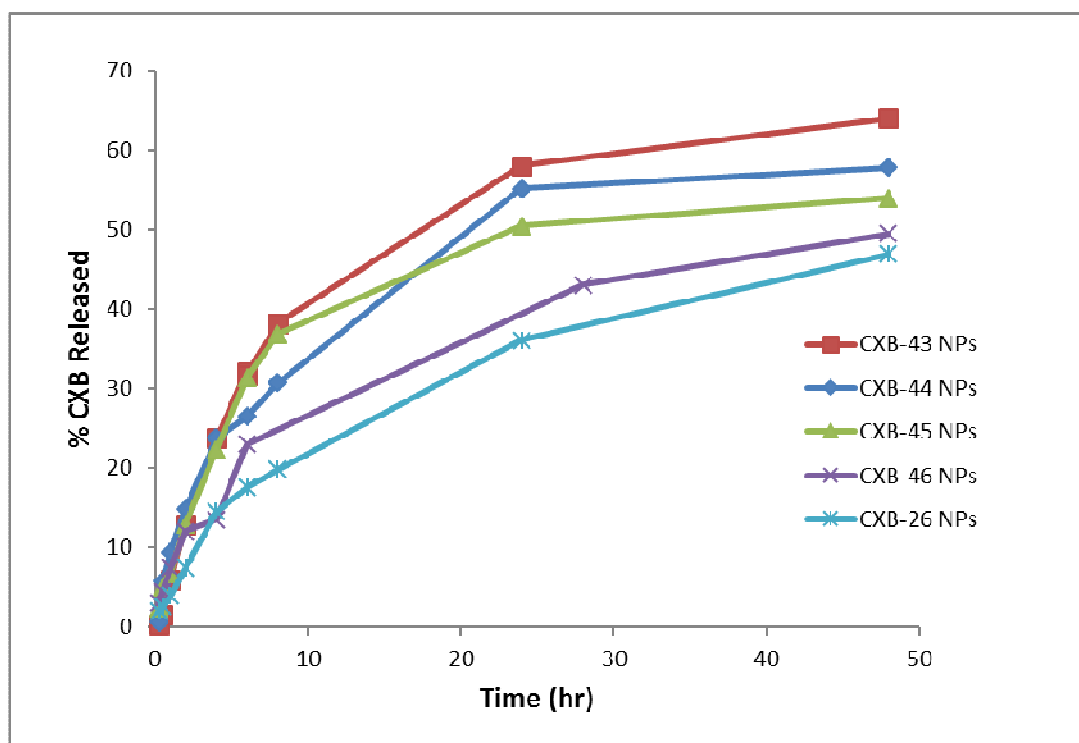


Figure 4: The in vitro release behavior of CXB from different polymeric NPs in PBS (pH 7.4) at 37°C.

A cytotoxic study was performed in order to assess the potential benefit of the polymeric NPs for enhancing the cytotoxic activity of CXB. The cytotoxicity of free CXB, and CXB-loaded polymeric NPs **CXB-43**, **CXB-45**, and **CXB-46** were assessed on human breast cancer cells, MCF-7, using MTT assay, a dye-based assay that depends on the metabolic activity of viable cells. In MTT assay, only metabolically active viable cells are able to convert the yellow MTT (3-(4,5-dimethylthiazol-2-yl)-2,5-diphenyl tetrazolium bromide) dye to purple MTT-formazan crystals which is further dissolved in solvent and analyzed spectrophotometrically.⁵⁸ Notably, free CXB, and CXB-loaded polymeric NPs **CXB-43**, **CXB-45**, and **CXB-46** demonstrated considerable reduction in cell viability in a dose-dependent manner (**Figure 5**). Questionably, the observed cytotoxic potential of CXB-loaded polymeric NPs **CXB-43**, **CXB-45**, and **CXB-46** (IC_{50} , 50% growth inhibition, 120, 100, and 52.5 $\mu\text{g}/\text{mL}$, respectively,

was lower than free drug solution (IC_{50} of 29.95 $\mu\text{g}/\text{mL}$) after 24 hr incubation period. The lower cytotoxicity demonstrated by NPs over 24 hr may be explained by the slow release of CXB from the formulated NPs which could be due to the hydrophobic-hydrophobic interaction between the drug and polymer.⁵⁹ Actually, the gradual slow release of CXB was confirmed by the results of in vitro drug release conducted in our study. Conclusively, CXB-loaded polymeric NPs developed in this study are expected to have high accumulation in tumor sites via the EPR effect and enhanced cellular uptake by nonspecific internalization into cells via endocytosis or phagocytosis.

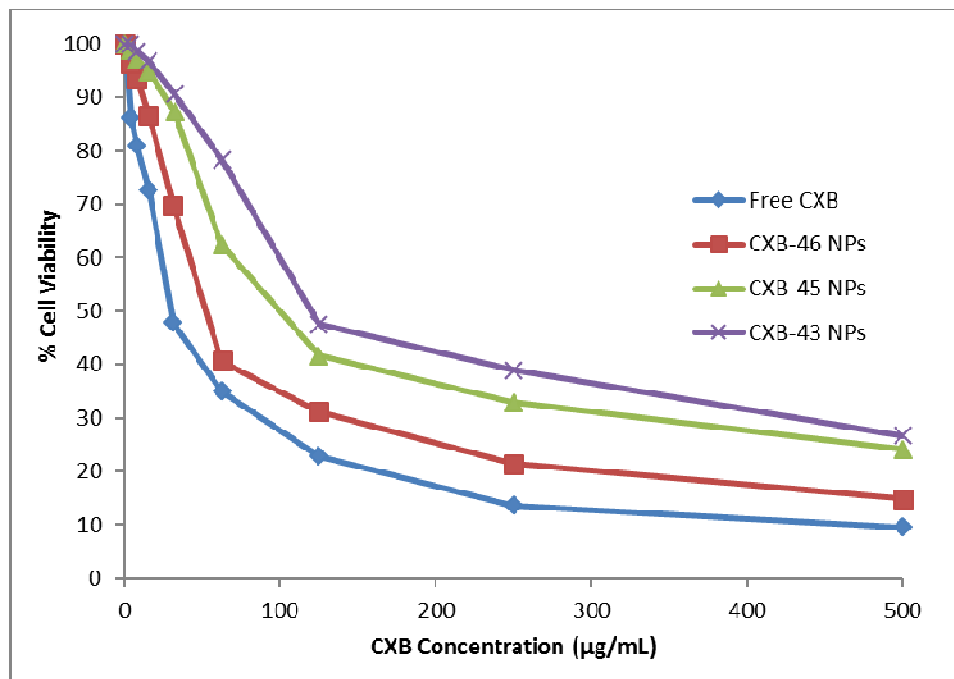


Figure 5: Cytotoxicity analysis of free CXB, and CXB-loaded polymeric NPs **CXB-43**, **CXB-45**, and **CXB-46** on MCF-7 cells at the concentration of 0-500 µg/mL after 24 hr.

Conclusions

The design of suitable polymeric materials is an increasingly important research area due to demands for applications in medicine as drug delivery systems. A new library of *s*-triazine polyamides, based on the reaction of *s*-triazine glycine and thioglycolic acid derivatives with ethylenediamine, benzidine, piperazine or *p*-phenylenediamine, was prepared. Structure-thermal property correlation based on changing the diacid residue as well as the amine residue at the triazine moiety, revealed the prepared polyamides with comparable thermal stabilities.

Thermal decomposition results revealed the thermal stability of the newly synthesized polyamides. In addition, all the polymers possess high activation energy values assigning their high stability. Most of the prepared polyamides exhibited a melting and glass transition peak indicating that most of the polymers are amorphous. The melting temperature, T_m , of all polymers ranged from 505°C to 643°C, which is an additional indication for the high stability of the polymers.

Biopolymeric nanoparticles based on the synthesized polyamides and loaded with the poorly soluble drug, CXB, were successfully developed. The nanoparticles exhibited small size and good colloidal stability together with a sustained drug release. Moreover, the nanoparticles were cytotoxic against breast cancer cells. Overall, these nanoparticles hold a great promise as drug delivery systems and are expected to accumulate significantly in tumor tissues via the EPR effect showing enhanced anti-tumor efficacy through maximizing the drugs anti-tumor efficacy and reducing systemic toxicity.

Experimental

Chemistry

Solvents and reagents were purchased from Sigma-Aldrich. Unless otherwise stated, the normal workup from organic solvent involved drying over Na_2SO_4 and rotary evaporation. TLC was performed using aluminum-backed Merck Silica Gel 60 F-254 plates using suitable solvent systems and spots being visualized by a Spectroline UV Lamp (254 or 365 nm) or I_2 vapor. Melting points were obtained in open capillary tubes using a MEL-Temp II melting point apparatus and are uncorrected. Infrared spectra (IR) were recorded on a

Perkin-Elmer 1600 series Fourier transform instrument as KBr pellets. The absorption bands (ν_{max}) are given in wave numbers (cm^{-1}). Nuclear magnetic resonance (NMR) spectra ($^1\text{H-NMR}$ and $^{13}\text{C-NMR}$) were recorded on a JEOL 500 MHz spectrometer at ambient temperature. Chemical shifts are reported in parts per million (ppm) and are referenced relative to residual solvent (e.g. CHCl_3 at δ 7.26 ppm for CDCl_3 , DMSO at δ 2.50 ppm for DMSO- d_6). Thermogravimetry (TG) and differential thermal analysis (DTA) and differential scanning calorimetry (DSC) analyses were carried out in the temperature range from 20°C to 700°C by LINSEIS STA PT1000 thermal analyzer. The experimental conditions were: alumina crucible, air atmosphere and heating rate 10°C/min. Elemental analyses were performed on a Perkin-Elmer 2400 elemental analyzer, and the values found were within $\pm 0.3\%$ of the theoretical values.

General Procedure of the preparation of triazine dicarboxylic acid monomers 9-14

Method A: A solution of cyanuric chloride **1** (1.84g, 10 mmol) in acetone (20 mL) was added dropwise to an ice-cold mixture of glycine **2**, thioglycolic acid **3** (20 mmol) and Na_2CO_3 (4.24 g, 40 mmol) in water (30 mL) during 30 min. The reaction mixture was stirred overnight at room temperature. The reaction mixture was neutralized with concentrated hydrochloric acid and filtered off, washed with cold water and dried to afford 2-chloro-4,6-disubstituted-1,3,5-triazine derivatives **4** and **5**.

To a stirred mixture of the crude **4** or **5** (3 mmol) and Na_2CO_3 solution (0.95 g, 9 mmol) in water (40 mL), morpholine **6**, piperidine **7** or aniline **8** (4.5mmol) in dioxane (20 mL) was added dropwise. The reaction mixture was stirred at 70–80°C for 8 h. The progress of the reaction was monitored by TLC. After the completion of the reaction, the reaction mixture was neutralized with hydrochloric acid. The product was filtered off, washed with cold water and recrystallized from ethanol to afford the triazine derivatives.

Method B: A solution of morpholine, piperidine or aniline (9 mmol) in dry CH_2Cl_2 was added dropwise to an ice-cold mixture of cyanuric chloride **1** (1.84 g, 10 mmol) and Na_2CO_3 (0.95 g, 9 mmol) in dry CH_2Cl_2 during 30 min. The reaction mixture was stirred for 30 min. The solid phase was filtered off, washed with CH_2Cl_2 . The solvent was evaporated under vacuum to dryness. The product was obtained as white solid and recrystallized from ethanol to afford 2,4-dichloro-6-substituted-1,3,5-triazine **12-14**.

To a stirred solution of 3crude **12-14** (8 mmol) in dioxane (20 mL), a mixture of glycine **2**, or thioglycolic acid **3** (24 mmol) and Na_2CO_3 (5.08 g, 48 mmol) in water (40 mL) was added dropwise. The reaction mixture was stirred at 70–80°C for 24 h. The progress of the reaction was monitored by TLC. After the completion of the reaction, the reaction mixture was neutralized with hydrochloric acid. The product was filtered off, washed with cold water and recrystallized from ethanol to afford the corresponding products.

2,2'-(6-Morpholino-1,3,5-triazine-2,4-diyl)bis(azanediy)diacetic acid 9. The product was obtained as a white powder, mp 258–260°C. **Method A:** 70% yield; **Method B:** 90% yield. IR (KBr): 3500–

2700 (br, OH, acid), 3324 (NH, amine), 1754 (C=O, acid) cm^{-1} . $^1\text{H-NMR}$ (500 MHz: DMSO- d_6): δ 3.53–3.55 (m, 8 H, 2 $\text{CH}_2\text{-N}$, 2 $\text{CH}_2\text{-O}$), 3.74–3.83 (m, 4 H, 2 $\text{CH}_2\text{-NH}$), 6.73–7.03 (m, 2 H, 2 NH, D_2O exchangeable), 12.25 (br s, 2 H, 2 COOH, D_2O exchangeable). Elemental analysis Calc. for $\text{C}_{11}\text{H}_{16}\text{N}_6\text{O}_5$: C, 42.31; H, 5.16; N, 26.91. Found: C, 42.47; H, 4.99; N, 26.67.

2,2'-(6-Morpholino-1,3,5-triazine-2,4-diyl)bis(sulfanediy)diacetic acid 10. The product was obtained as a white powder, mp 190–192°C. **Method A:** 91% yield. IR (KBr): 3459–2500 (br, OH, acid), 1718 (C=O, acid) cm^{-1} . $^1\text{H-NMR}$ (500 MHz: DMSO- d_6): δ 3.54–3.56 (m, 6 H, 2 CH_2O , $\text{CH}_2\text{-S}$), 3.63–3.65 (m, 4 H, 2 CH_2N), 3.72 (s, 2 H, $\text{CH}_2\text{-S}$), 12.43 (br s, 2 H, 2 COOH, D_2O exchangeable). Elemental analysis: Calc. for $\text{C}_{11}\text{H}_{14}\text{N}_4\text{O}_5\text{S}_2$: C, 38.14; H, 4.07; N, 16.17. Found: C, 37.98; H, 4.21; N, 16.04.

2,2'-(6-(Piperidin-1-yl)-1,3,5-triazine-2,4-diyl)bis(azanediy)diacetic acid 11. The product was obtained as a white powder, mp 248–250°C. **Method A:** 87% yield. IR (KBr): 3500–2500 (br, OH, acid), 3290 (NH, amine), 1745 (C=O, acid) cm^{-1} . $^1\text{H-NMR}$ (500 MHz: DMSO- d_6): δ 1.39 (s, 4 H, 2 CH_2), 1.54 (s, 2 H, CH_2), 3.77–3.79 (m, 8 H, 2 $\text{CH}_2\text{-N}$, 2 $\text{CH}_2\text{-NH}$), 6.75–6.91 (m, 2H, 2NH, D_2O exchangeable), 12.11 (br s, 2 H, 2 COOH, D_2O exchangeable). $^{13}\text{C-NMR}$ (125 MHz: DMSO- d_6): δ 24.83, 25.82, 42.66, 43.93, 164.29, 165.92, 166.20, 172.69, 172.75. Elemental analysis Calc. for $\text{C}_{12}\text{H}_{18}\text{N}_6\text{O}_4$: C, 46.45; H, 5.85; N, 27.08. Found: C, 46.21; H, 6.01; N, 27.19.

2,2'-(6-(Piperidin-1-yl)-1,3,5-triazine-2,4-diyl)bis(sulfanediy)diacetic acid 12. The product was obtained as a white powder, mp 155–157°C. **Method A:** 85% yield. IR (KBr): 3440–2500 (br, OH, acid), 1716 (C=O, acid) cm^{-1} . $^1\text{H-NMR}$ (500 MHz: DMSO- d_6): δ 1.42 (s, 4 H, 2 CH_2), 1.55 (br s, 2 H, CH_2), 3.60–3.68 (m, 4 H, 2 CH_2), 3.69 (s, 2 H, $\text{CH}_2\text{-S}$), 3.78 (s, 2 H, $\text{CH}_2\text{-S}$), 12.59 (br s, 2 H, 2 COOH, D_2O exchangeable). $^{13}\text{C-NMR}$ (125 MHz: DMSO- d_6): δ 24.53, 25.60, 33.10, 44.52, 162.66, 170.91, 171.01, 177.78, 177.85. Elemental analysis Calc. for $\text{C}_{12}\text{H}_{16}\text{N}_4\text{O}_4\text{S}_2$: C, 41.85; H, 4.68; N, 16.27. Found: C, 41.59; H, 4.98; N, 16.34.

2,2'-(6-(Phenylamino)-1,3,5-triazine-2,4-diyl)bis(azanediy)diacetic acid 13. The product was obtained as a white powder, mp 258–260°C. **Method B:** 90% yield. IR (KBr): 3500–2700 (br, OH, acid), 3451 (NH, amine), 1638 (C=O, acid) cm^{-1} . $^1\text{H-NMR}$ (500 MHz: DMSO- d_6): δ 3.88 (br s, 4 H, 2 CH_2), 6.87 (t, 1 H, $J = 7.7$ Hz, Ar-H), 6.93–7.14 (m, 2 H, 2 NH, D_2O exchangeable), 7.17 (t, 2 H, $J = 7.7$ Hz, 2 Ar-H), 7.65–7.69 (m, 2 H, 2 Ar-H), 8.98–9.04 (m, 1 H, NH, D_2O exchangeable), 12.44 (br s, 2 H, 2 COOH, D_2O exchangeable). Elemental analysis Calc. for $\text{C}_{13}\text{H}_{14}\text{N}_6\text{O}_4$: C, 49.06; H, 4.43; N, 26.40. Found: C, 49.15; H, 4.22; N, 26.17.

2,2'-(6-(Phenylamino)-1,3,5-triazine-2,4-diyl)bis(sulfanediy)diacetic acid 14. The product was obtained as a white powder, mp 257–258°C. **Method B:** 90% yield. IR (KBr): 3500–2600 (br, OH, acid), 3449 (NH, amine), 1752 (C=O, acid) cm^{-1} . $^1\text{H-NMR}$ (500 MHz: DMSO- d_6): δ 3.93 (s, 4 H, 2 CH_2), 6.99–7.08 (m, 1 H, Ar-H), 7.25–7.36 (m, 2 H, 2 Ar-H), 7.56 (d, 2H, $J = 6.9$ Hz, 2 Ar-H), 9.72 (s, 1 H, NH, D_2O exchangeable), 10.68 (br. s, 2 H, 2 COOH, D_2O exchangeable).

ARTICLE

Journal Name

Elemental analysis Calc. for $C_{13}H_{12}N_4O_4S_2$: C, 44.31; H, 3.43; N, 15.90. Found: C, 44.53; H, 3.39; N, 15.75.

Synthesis of (6-substituted-1,3,5-triazin-2,4-yl)bissubstituted diacetyl chloride derivatives 15-20

A mixture of (1.0 mmol) (6-substituted-1,3,5-triazin-2,4-yl)bissubstituted diacetic acid derivatives 9-14 and (5 mL) thionyl chloride in 10 mL dichloromethane was stirred continuously where the temperature was maintained at 10°C for 30 min. The reaction mixture temperature was raised to 80°C and refluxed for 8 h. The solvent and volatiles were removed under reduced pressure and the crude residue was washed thoroughly with hexane to produce the desired (6-substituted-1,3,5-triazin-2,4-yl)bissubstituted diacetyl chloride derivatives 15-20. The crude residue was used directly to the next step.

General method of polymerization

To a stirred cold (ice-bath) solution of (1.0 mmol) diamine (ethylenediamine 21, benzidine 22, piperazine 23 or *p*-phenylenediamine 24) in 3 mL DMF, (0.41 mL, 3 mmol) triethylamine was added. A solution of (1.0 mmol) of the previously prepared (6-substituted-1,3,5-triazin-2,4-yl)bissubstituted diacetyl chloride derivatives 15-20 in (3 mL) DMF was added dropwise for 30 min. The reaction mixture was stirred overnight and was then poured into ice cold water. The formed polymer was filtered, washed thoroughly with water, ethanol, and air dried.

Poly[2-(4-(2-(2-aminoethylamino)-2-oxoethylamino)-6-morpholino-1,3,5-triazin-2-ylamino)acetic acid] 25. The polymer 25 was obtained as brown solid from copolymerization of ethylenediamine 21 and 2,2'-(6-morpholino-1,3,5-triazin-2,4-diy)bis(azanediyl)diacetyl chloride 15, yield 86%; mp over 300°C. IR (KBr): 3389 (NH), 2965, 2860 (sp^3 -CH), 1674 (C=O, amide) cm^{-1} . Elemental analysis: Calculated for $C_{13}H_{20}N_8O_3$: C, 46.42; H, 5.99; N, 33.31. Found: C, 46.10; H, 6.11; N, 32.99.

Poly[2-(4-(2-(2-aminoethylamino)-2-oxoethylthio)-6-morpholino-1,3,5-triazin-2-ylthio)acetic acid] 26. The polymer 26 was obtained as black solid from copolymerization of ethylenediamine 21 and 2,2'-(6-morpholino-1,3,5-triazin-2,4-diy)bis(sulfanediyl)diacetyl chloride 16, yield 76%; mp over 300°C. IR (KBr): 3433 (NH), 2922, 2857 (sp^3 -CH), 1652 (C=O, amide) cm^{-1} . Elemental analysis: Calculated for $C_{13}H_{18}N_6O_3S_2$: C, 42.15; H, 4.90; N, 22.69. Found: C, 41.85; H, 4.97; N, 22.37.

Poly[2-(4-(2-(2-aminoethylamino)-2-oxoethylamino)-6-(piperidin-1-yl)-1,3,5-triazin-2-ylamino)acetic acid] 27. The polymer 27 was obtained as brown solid from copolymerization of ethylenediamine 21 and 2,2'-(6-(piperidin-1-yl)-1,3,5-triazin-2,4-diy)bis(azanediyl)diacetyl chloride 17, yield 87%; mp over 300°C. IR (KBr): 3418 (NH), 2933, 2858 (sp^3 -CH), 1663 (C=O, amide) cm^{-1} . Elemental analysis: Calculated for $C_{14}H_{22}N_8O_2$: C, 50.29; H, 6.63; N, 33.51. Found: C, 49.96; H, 6.68; N, 33.23.

Poly[2-(4-(2-(2-aminoethylamino)-2-oxoethylthio)-6-(piperidin-1-yl)-1,3,5-triazin-2-ylthio)acetic acid] 28. The polymer 28 was obtained as dark brown solid from copolymerization of

ethylenediamine 21 and 2,2'-(6-(piperidin-1-yl)-1,3,5-triazin-2,4-diy)bis(sulfanediyl)diacetyl chloride 18, yield 68%; mp over 300°C. IR (KBr): 3385 (NH), 2931, 2855 (sp^3 -CH), 1652 (C=O, amide) cm^{-1} . Elemental analysis: Calculated for $C_{14}H_{20}N_6O_2S_2$: C, 45.63; H, 5.47; N, 22.81. Found: C, 45.35; H, 5.56; N, 22.63.

Poly[2-(4-(2-(2-aminoethylamino)-2-oxoethylamino)-6-(phenylamino)-1,3,5-triazin-2-ylamino)acetic acid] 29. The polymer 29 was obtained as dark brown solid from copolymerization of ethylenediamine 21 and 2,2'-(6-(phenylamino)-1,3,5-triazin-2,4-diy)bis(azanediyl)diacetyl chloride 19, yield 70%; mp over 300°C. IR (KBr): 3379 (NH), 2927, 2850 (sp^3 -CH), 1641 (C=O, amide) cm^{-1} . Elemental analysis: Calculated for $C_{15}H_{18}N_6O_2$: C, 52.62; H, 5.30; N, 32.73. Found: C, 52.28; H, 5.37; N, 32.47.

Poly[2-(4-(2-(2-aminoethylamino)-2-oxoethylthio)-6-(phenylamino)-1,3,5-triazin-2-ylthio)acetic acid] 30. The polymer 30 was obtained as yellow solid from copolymerization of ethylenediamine 21 and 2,2'-(6-(phenylamino)-1,3,5-triazin-2,4-diy)bis(sulfanediyl)diacetyl chloride 20, yield 77%; mp over 300°C. IR (KBr): 3410 (NH), 2925, 2857 (sp^3 -CH), 1683 (C=O, amide) cm^{-1} . Elemental analysis: Calculated for $C_{15}H_{16}N_6O_2S_2$: C, 47.86; H, 4.28; N, 22.32. Found: C, 47.51; H, 4.32; N, 22.02.

Poly[2-(4-(2-(4'-aminobiphenyl-4-ylamino)-2-oxoethylamino)-6-morpholino-1,3,5-triazin-2-ylamino)acetic acid] 31. The polymer 31 was obtained as black solid from copolymerization of benzidine 22 and 2,2'-(6-morpholino-1,3,5-triazin-2,4-diy)bis(azanediyl)diacetyl chloride 15, yield 80%; mp over 300°C. IR (KBr): 3431 (NH), 2956, 2924, 2858 (sp^3 -CH), 1652 (C=O, amide) cm^{-1} . Elemental analysis: Calculated for $C_{23}H_{24}N_8O_3$: C, 59.99; H, 5.25; N, 24.33. Found: C, 59.61; H, 5.32; N, 24.01.

Poly[2-(4-(2-(4'-aminobiphenyl-4-ylamino)-2-oxoethylthio)-6-morpholino-1,3,5-triazin-2-ylthio)acetic acid] 32. The polymer 32 was obtained as black solid from copolymerization of benzidine 22 and 2,2'-(6-morpholino-1,3,5-triazin-2,4-diy)bis(sulfanediyl)diacetyl chloride 16, yield 73%; mp over 300°C. IR (KBr): 3445 (NH), 2963, 2911, 2855 (sp^3 -CH), 1637 (C=O, amide) cm^{-1} . Elemental analysis: Calculated for $C_{23}H_{22}N_6O_3S_2$: C, 55.85; H, 4.48; N, 16.99. Found: C, 55.51; H, 4.54; N, 16.61.

Poly[2-(4-(2-(4'-aminobiphenyl-4-ylamino)-2-oxoethylamino)-6-(piperidin-1-yl)-1,3,5-triazin-2-ylamino)acetic acid] 33. The polymer 33 was obtained as greenish yellow solid from copolymerization of benzidine 22 and 2,2'-(6-(piperidin-1-yl)-1,3,5-triazin-2,4-diy)bis(azanediyl)diacetyl chloride 17, yield 74%; mp over 300°C. IR (KBr): 3425 (NH), 2964, 2856 (sp^3 -CH), 1674 (C=O, amide) cm^{-1} . Elemental analysis: Calculated for $C_{24}H_{26}N_8O_2$: C, 62.87; H, 5.72; N, 24.44. Found: C, 62.53; H, 5.82; N, 24.13.

Poly[2-(4-(2-(4'-aminobiphenyl-4-ylamino)-2-oxoethylthio)-6-(piperidin-1-yl)-1,3,5-triazin-2-ylthio)acetic acid] 34. The polymer 34 was obtained as greenish yellow solid from copolymerization of benzidine 22 and 2,2'-(6-(piperidin-1-yl)-1,3,5-triazin-2,4-diy)bis(sulfanediyl)diacetyl chloride 18, yield 77%; mp over 300°C. IR (KBr): 3432 (NH), 2931, 2853 (sp^3 -CH), 1688 (C=O, amide) cm^{-1} .

Elemental analysis: Calculated for $C_{24}H_{24}N_6O_2S_2$: C, 58.52; H, 4.91; N, 17.06. Found: C, 58.20; H, 4.97; N, 16.88.

Poly[2-(4-(2-(4'-aminobiphenyl-4-ylamino)-2-oxoethylamino)-6-(phenyl amino)-1,3,5-triazin-2-ylamino)acetic acid] 35. The polymer **35** was obtained as black solid from copolymerization of benzidine **22** and 2,2'-(6-(phenylamino)-1,3,5-triazine-2,4-diy)bis(azanediy)diacetyl chloride **19**, yield 73%; mp over 300°C. IR (KBr): 3374 (NH), 2975, 2950 (sp^3 -CH), 1613 (C=O, amide) cm^{-1} . Elemental analysis: Calculated for $C_{25}H_{22}N_8O_2$: C, 64.37; H, 4.75; N, 24.02. Found: C, 64.03; H, 4.87; N, 23.91.

Poly[2-(4-(2-(4'-aminobiphenyl-4-ylamino)-2-oxoethylthio)-6-(phenyl amino)-1,3,5-triazin-2-ylthio)acetic acid] 36. The polymer **36** was obtained as brown solid from copolymerization of benzidine **22** and 2,2'-(6-(phenylamino)-1,3,5-triazine-2,4-diy)bis(sulfanediy)diacetyl chloride **20**, yield 78%; mp over 300°C. IR (KBr): 3403 (NH), 2926, 2850 (sp^3 -CH), 1733 (C=O, amide) cm^{-1} . Elemental analysis: Calculated for $C_{25}H_{20}N_6O_2S_2$: C, 59.98; H, 4.03; N, 16.79. Found: C, 59.62; H, 4.12; N, 16.46.

Poly[2-(4-morpholino-6-(2-oxo-2-(piperazin-1-yl)ethylamino)-1,3,5-triazin-2-ylamino)acetic acid] 37. The polymer **37** was obtained as brown solid from copolymerization of piperazine **23** and 2,2'-(6-morpholino-1,3,5-triazine-2,4-diy)bis(azanediy)diacetyl chloride **15**, yield 77%; mp over 300°C. IR (KBr): 3434 (NH), 2924, 2857 (sp^3 -CH), 1620 (C=O, amide) cm^{-1} . Elemental analysis: Calculated for $C_{15}H_{22}N_6O_3$: C, 49.71; H, 6.12; N, 30.92. Found: C, 49.42; H, 6.18; N, 30.64.

Poly[2-(4-morpholino-6-(2-oxo-2-(piperazin-1-yl)ethylthio)-1,3,5-triazin-2-ylthio)acetic acid] 38. The polymer **38** was obtained as greenish yellow solid from copolymerization of piperazine **23** and 2,2'-(6-morpholino-1,3,5-triazine-2,4-diy)bis(sulfanediy)diacetyl chloride **16**, 0.29 g (73%) yield; mp over 300°C. IR (KBr): 3439 (NH), 2964, 2919, 2857 (sp^3 -CH), 1652 (C=O, amide) cm^{-1} . Elemental analysis: Calculated for $C_{15}H_{20}N_6O_3S_2$: C, 45.44; H, 5.08; N, 21.20. Found: C, 45.08; H, 5.17; N, 20.94.

Poly[2-(4-(2-oxo-2-(piperazin-1-yl)ethylamino)-6-(piperidin-1-yl)-1,3,5-triazin-2-ylamino)acetic acid] 39. The polymer **39** was obtained as buff solid from copolymerization of piperazine **23** and 2,2'-(6-(piperidin-1-yl)-1,3,5-triazine-2,4-diy)bis(azanediy)diacetyl chloride **17**, 0.30 g (83%) yield; mp over 300°C. IR (KBr): 3428 (NH), 2971, 2931, 2860 (sp^3 -CH), 1641 (C=O, amide) cm^{-1} . Elemental analysis: Calculated for $C_{16}H_{24}N_8O_2$: C, 53.32; H, 6.71; N, 31.09. Found: C, 53.01; H, 6.79; N, 30.83.

Poly[2-(4-(2-oxo-2-(piperazin-1-yl)ethylthio)-6-(piperidin-1-yl)-1,3,5-triazin-2-ylthio)acetic acid] 40. The polymer **40** was obtained as brown solid from copolymerization of piperazine **23** and 2,2'-(6-(piperidin-1-yl)-1,3,5-triazine-2,4-diy)bis(sulfanediy)diacetyl chloride **18**, yield 71%; mp over 300°C. IR (KBr): 3440 (NH), 2931, 2853 (sp^3 -CH), 1630 (C=O, amide) cm^{-1} . Elemental analysis: Calculated for $C_{16}H_{22}N_6O_2S_2$: C, 48.71; H, 5.62; N, 21.30. Found: C, 48.34; H, 5.66; N, 20.97.

Poly[2-(4-(2-oxo-2-(piperazin-1-yl)ethylamino)-6-(phenylamino)-1,3,5-triazin-2-ylamino)acetic acid] 41. The polymer **41** was

obtained as brown solid from copolymerization of piperazine **23** and 2,2'-(6-(phenylamino)-1,3,5-triazine-2,4-diy)bis(azanediy)diacetyl chloride **19**, yield 79%; mp over 300°C. IR (KBr): 3388 (NH), 2975, 2925 (sp^3 -CH), 1615 (C=O, amide) cm^{-1} . Elemental analysis: Calculated for $C_{17}H_{20}N_8O_2$: C, 55.43; H, 5.47; N, 30.42. Found: C, 55.18; H, 5.52; N, 30.13.

Poly[2-(4-(2-oxo-2-(piperazin-1-yl)ethylthio)-6-(phenylamino)-1,3,5-triazin-2-ylthio)acetic acid] 42. The polymer **42** was obtained as brown solid from copolymerization of piperazine **23** and 2,2'-(6-(phenylamino)-1,3,5-triazine-2,4-diy)bis(sulfanediy)diacetyl chloride **20**, yield 80%; mp over 300°C. IR (KBr): 3414 (NH), 2925, 2857 (sp^3 -CH), 1622 (C=O, amide) cm^{-1} . Elemental analysis: Calculated for $C_{17}H_{18}N_6O_2S_2$: C, 50.73; H, 4.51; N, 20.88. Found: C, 50.44; H, 4.61; N, 20.53.

Poly[2-(4-(2-(4-aminophenylamino)-2-oxoethylamino)-6-morpholino-1,3,5-triazin-2-ylamino)acetic acid] 43. The polymer **43** was obtained as black solid from copolymerization of *p*-phenylenediamine **24** and 2,2'-(6-morpholino-1,3,5-triazine-2,4-diy)bis(azanediy)diacetyl chloride **15**, yield 75%; mp over 300°C. IR (KBr): 3425 (NH), 2968, 2859 (sp^3 -CH), 1601 (C=O, amide) cm^{-1} . Elemental analysis: Calculated for $C_{17}H_{20}N_8O_3$: C, 53.12; H, 5.24; N, 29.15. Found: C, 52.80; H, 5.28; N, 28.86.

Poly[2-(4-(2-(4-aminophenylamino)-2-oxoethylthio)-6-morpholino-1,3,5-triazin-2-ylthio)acetic acid] 44. The polymer **44** was obtained as greenish brown solid from copolymerization of *p*-phenylenediamine **24** and 2,2'-(6-morpholino-1,3,5-triazine-2,4-diy)bis(sulfanediy)diacetyl chloride **16**, yield 76%; mp over 300°C. IR (KBr): 3437 (NH), 2916, 2858 (sp^3 -CH), 1674 (C=O, amide) cm^{-1} . Elemental analysis: Calculated for $C_{17}H_{18}N_6O_3S_2$: C, 48.79; H, 4.34; N, 20.08. Found: C, 48.41; H, 4.46; N, 19.87.

Poly[2-(4-(2-(4-aminophenylamino)-2-oxoethylamino)-6-(piperidin-1-yl)-1,3,5-triazin-2-ylamino)acetic acid] 45. The polymer **45** was obtained as brown solid from copolymerization of *p*-phenylenediamine **24** and 2,2'-(6-(piperidin-1-yl)-1,3,5-triazine-2,4-diy)bis(azanediy)diacetyl chloride **17**, yield 86%; mp over 300°C. IR (KBr): 3365 (NH), 2932, 2857 (sp^3 -CH), 1605 (C=O, amide) cm^{-1} . Elemental analysis: Calculated for $C_{18}H_{22}N_8O_2$: C, 56.53; H, 5.80; N, 29.30. Found: C, 56.21; H, 5.86; N, 28.98.

Poly[2-(4-(2-(4-aminophenylamino)-2-oxoethylthio)-6-(piperidin-1-yl)-1,3,5-triazin-2-ylthio)acetic acid] 46. The polymer **46** was obtained as yellow solid from copolymerization of *p*-phenylenediamine **24** and 2,2'-(6-(piperidin-1-yl)-1,3,5-triazine-2,4-diy)bis(sulfanediy)diacetyl chloride **18**, yield 86%; mp over 300°C. IR (KBr): 3424 (NH), 2931, 2853 (sp^3 -CH), 1698 (C=O, amide) cm^{-1} . Elemental analysis: Calculated for $C_{18}H_{20}N_6O_2S_2$: C, 51.90; H, 4.84; N, 20.18. Found: C, 51.69; H, 4.87; N, 19.92.

Poly[2-(4-(2-(4-aminophenylamino)-2-oxoethylamino)-6-(phenylamino)-1,3,5-triazin-2-ylamino)acetic acid] 47. The polymer **47** was obtained as dark brown solid from copolymerization of *p*-phenylenediamine **24** and 2,2'-(6-(phenylamino)-1,3,5-triazine-2,4-diy)bis(azanediy)diacetyl chloride **19**, yield 69%; mp over 300°C. IR (KBr): 3348 (NH), 2950, 2875 (sp^3 -CH), 1614 (C=O, amide) cm^{-1} .

ARTICLE

Journal Name

Elemental analysis: Calculated for $C_{19}H_{18}N_8O_2$: C, 58.45; H, 4.65; N, 28.70. Found: C, 58.12; H, 4.78; N, 28.42.

Poly[2-(4-(2-(4-aminophenylamino)-2-oxoethylthio)-6-(phenylamino)-1,3,5-triazin-2-ylthio)acetic acid] 48. The polymer **48** was obtained as dark brown solid from copolymerization of *p*-phenylenediamine **24** and 2,2'-(6-(phenylamino)-1,3,5-triazine-2,4-diylo)bis(sulfanediyl)diacetyl chloride **20**, yield 68%; mp over 300°C. IR (KBr): 3358 (NH), 2950, 2900 (sp^3 -CH), 1609 (C=O, amide) cm^{-1} . Elemental analysis: Calculated for $C_{19}H_{16}N_6O_2S_2$: C, 53.79; H, 3.80; N, 19.80. Found: C, 53.45; H, 3.98; N, 19.59.

Biology**Preparation of drug-loaded polymeric nanoparticles**

Celecoxib (CXB)-loaded polymeric NPs were prepared by nanoprecipitation (solvent displacement) method.⁵¹ In brief, 50 mg polymer and 10 mg CXB were dissolved in 3 mL dimethyl sulfoxide (DMSO). The organic solvent containing drug and polymer was injected dropwise into 50 mL water consisting 1 % w/v pluronic F-68 under bath sonication for 30 min. The resultant nanosuspension was centrifuged at 17000 rpm at 4°C for 30 min (Sigma laboratory refrigerated centrifuge, model 3K-30, Germany) in order to separate the NPs. The sedimented NPs were washed with distilled water, reconstituted in 5 mL distilled water and then freeze-dried (CRYODOS-50 Freeze-drier, Telstar, Spain). Blank NPs were also prepared in the same method omitting CXB.

Physicochemical characterization of nanoparticles

Drug content: The amount of CXB encapsulated in the polymeric NPs was determined by both direct and indirect methods. In the direct method, 10 mg lyophilized NPs were dissolved in 5 mL methanol with the aid of ultrasonication for 10 min, then filtered through 0.45 μm membrane filter and analyzed for free CXB via HPLC. In the indirect method, after ultracentrifugation of the bulk suspension at 17,000 rpm for 30 min, the supernatant was analyzed for free CXB concentration via HPLC. All the analysis was performed in triplicate.

A reverse phase HPLC method was used for quantifying CXB.⁶⁰ HPLC analysis was carried out with Agilent 1200 chromatograph using an Eclipse plus C18 column (3.5 μm 4.6 x 100 mm), and PDA detector. An isocratic solvent system consisting of 70:30 (v/v) methanol-acidified water (phosphoric acid, pH = 4) was used at a flow rate of 1.0 mL/min and an injection volume of 10 μL , and the peaks were detected at 250 nm.

Particle size distribution and zeta potential: The NPs size distribution and zeta potential were determined using dynamic light scattering (DLS) technique with a NanoZS/ZEN3600 Zetasizer (Malvern Instruments Ltd., UK) with the non-invasive backscattering technology at a detection angle of 173° after at least 200-fold dilution with purified water. All of the DLS measurements were performed at 25.0 \pm 0.1°C at 20s intervals for three repeat measurements. For the zeta potential measurement, each diluted nanosuspension (1 mL) was put in a universal folded capillary cell equipped with platinum electrodes. The electrophoresis mobility

was measured and the zeta potential was calculated by the Dispersion Technology Software provided by Malvern.

Morphological analysis: Transmission electron microscopy (TEM, JEM-100 CX, JEOL, Japan) was performed to elucidate the morphology of CXB-loaded polymeric NPs. A 50-fold diluted dispersion of NPs in distilled water was deposited onto a carbon grid. After 30 s, the dispersion was stained with uranyl acetate solution for 1 min. The excess solution was drawn off with a filter paper, and the sample was dried at room temperature.

Fourier Transform Infrared (FTIR) Spectroscopy: The FTIR spectra of free CXB, and CXB-loaded polymeric nanoparticles were recorded using a Spectrum RXI FTIR spectrometer (Perkin Elmer, USA). Samples were finely grounded with IR grade KBr and then pressed into pellet, and IR spectra were taken in transmission over the range of 4000–500 cm^{-1} at ambient temperature

In vitro drug release: The in vitro release of CXB from polymeric NPs was performed using dialysis bag. Freshly prepared nanosuspension (equivalent to 2 mg/mL of CXB) was placed in a dialysis bag (cut-off 12–14 kDa, Spectrum Laboratories, Inc, Rancho Dominguez, CA, USA). The bag was then suspended in a beaker containing 100 mL of phosphate buffered saline (PBS, pH 7.4) with SLS (0.5% w/v). This assembly was kept in an oscillating thermostatic water bath (Julabo, Germany) maintained at 100 rpm and 37°C \pm 0.5°C. At regular time intervals, 2 mL of CXB releasing media was withdrawn and replaced with an equal volume of fresh releasing medium to maintain sink conditions. All the samples were filtered through 0.45 μm membrane filter and analyzed for CXB content using HPLC method.

In vitro cytotoxicity: Cytotoxicity was determined by classic MTT assay. Briefly, MCF-7 breast cancer cells were seeded in 96-well plate at concentration of 5 \times 10³ cells/well in Dulbecco's modified eagle medium (DMEM) enriched with 10% fetal bovine serum and cultured overnight. Free drug solution and drug loaded polymeric NPs **CXB-43**, **CXB-45**, and **CXB-46** were added to reach a final concentration of 500 $\mu g/mL$, and incubated for 24 hr. Measurement was performed in microplate reader (Model 550, Bio-Rad, USA).

Acknowledgements

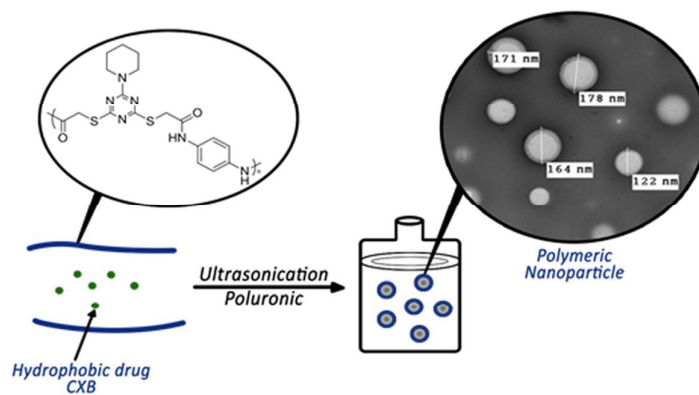
The authors thank Alexandria University-Research Enhancement Program (ALEXREP), for funding this work through the Research Project (HLTH-13 +BASC-13).

Notes and references

- 1 S. W. Shalaby, Y. Ykada, R. Langer and J. Williams, *Polymers of Biological and Biomedical Significance*, American Chemical Society, Washington, DC, 1994, vol. 540.
- 2 M. Chasin and R. Langer, *Biodegradable polymers as drug delivery systems*, Marcel Dekker Inc., New York, 1990, vol. 45.
- 3 K. E. Gonsalves and P. M. Mungara, *Synth. Prop. Degrad. Polyam. Relat. Polym. Trends Polym. Sci.*, 1996, **1**, 25–31.
- 4 M. Martina and D. W. Hutmacher, *Polym. Int.*, 2007, **56**,

- 145–157.
- 5 S. Bechaouch, B. Coutin and H. Sekiguchi, *Macromol. Chem. Phys.*, 1996, **197**, 1661–1668.
- 6 S. Bechaouch, I. Gachard, B. Coutin and H. Sekiguchi, *Polym. Bull.*, 1997, **38**, 365–370.
- 7 S. Pascual, I. Gachard, B. Coutin and H. Sekiguchi, *Macromol. Chem. Phys.*, 2001, **202**, 873–881.
- 8 A. Almontassir, S. Gesti, L. Franco and J. Puiggali, *Macromolecules*, 2004, **37**, 5300–5309.
- 9 M. J. Kottke and M. R. Edward, *Tablet Dosage Forms. In: Banker GS*, 2002.
- 10 A. S. Alam and E. L. Parrott, *J. Pharm. Sci.*, 1971, **60**, 263–266.
- 11 V. B. Kotwal, M. Saifee, N. Inamdar and K. Bhise, *Indian J. Pharm.*, 2007, **69**, 616–625.
- 12 L. S. Nair and C. T. Laurencin, *Prog. Polym. Sci.*, 2007, **32**, 762–798.
- 13 Y. Wang, G. A. Ameer, B. J. Sheppard and R. Langer, *Nat. Biotechnol.*, 2002, **20**, 602–606.
- 14 M. Vert, *Biomacromolecules*, 2005, **6**, 538–546.
- 15 L. Zhang, C. Xiong and X. Deng, *J. Appl. Polym. Sci.*, 1995, **56**, 103–112.
- 16 A. Göpferich, *Biomaterials*, 1996, **17**, 103–114.
- 17 D. Eglin, D. Mortisen and M. Alini, *Soft Matter*, 2009, **5**, 938–947.
- 18 K. Hemmrich, J. Salber, M. Meersch, U. Wiesemann, T. Gries, N. Pallua and D. Klee, *J. Mater. Sci. Mater. Med.*, 2008, **19**, 257–267.
- 19 N. Paredes, A. Rodríguez-Galán and J. Puiggali, *Polymer (Guildf.)*, 1996, **37**, 4175–4181.
- 20 J. M. Anderson, D. F. Gibbons, R. L. Martin, A. Hiltner and R. Woods, *J. Biomed. Mater. Res.*, 1974, **8**, 197–207.
- 21 A. S. Gupta and S. T. Lopina, *J. Biomater. Sci. Polym. Ed.*, 2002, **13**, 1093–1104.
- 22 L. H. Ho and S. J. Huang, *Polym. Prepr. Am. Chem. Soc. Div. Polym. Chem.*, 1992, **33**, 94–95.
- 23 N. Paredes, A. Rodríguez-Galán and J. Puiggali, *J. Polym. Sci. Part A Polym. Chem.*, 1998, **36**, 1271–1282.
- 24 N. Paredes, M. T. Casas, J. Puiggali and B. Lotz, *J. Polym. Sci. Part B Polym. Phys.*, 1999, **37**, 2521–2533.
- 25 N. Paredes, A. Rodríguez-Galán, J. Puiggali and C. Peraire, *J. Appl. Polym. Sci.*, 1998, **69**, 1537–1549.
- 26 A. Rodríguez, Galán, M. Pelfort, J. E. Aceituno and J. Puiggali, *J. Appl. Polym. Sci.*, 1999, **74**, 2312–2320.
- 27 N. Arabuli, G. Tsitlanadze, L. Edilashvili, D. Kharadze, T. Gogvadze, V. Beridze, Z. Gomurashvili and R. Katsarava, *Macromol. Chem. Phys.*, 1994, **195**, 2279–2289.
- 28 R. Katsarava, V. Beridze, N. Arabuli, D. Kharadze, C. C. Chu and C. Y. Won, *J. Polym. Sci. Part A Polym. Chem.*, 1999, **37**, 391–407.
- 29 Z. Gomurashvili, H. R. Kricheldorf and R. Katsarava, *J. Macromol. Sci. Part A Pure Appl. Chem.*, 2000, **37**, 215–227.
- 30 S. Jin, P. M. Mungara and K. E. Gonsalves, *J. Polym. Sci. Part A Polym. Chem.*, 1997, **35**, 499–507.
- 31 M. Yoshida, M. Asano, M. Kumakura, R. Katakai, T. Mashimo, H. Yuasa and H. Yamanaka, *Eur. Polym. J.*, 1991, **27**, 325–329.
- 32 B. Bianco, L. Castaldo, A. del Gaudio, G. Maglio, R. Palumbo, F. La Cara, G. Peluso and O. Petillo, *Polym. Bull.*, 1997, **39**, 279–286.
- 33 L. Castaldo, P. Corbo, G. Maglio and R. Palumbo, *Polym. Bull.*, 1992, **28**, 301–307.
- 34 S. T. Asundaria and K. C. Patel, *Int. J. Polym.*, 2010, **59**, 370–386.
- 35 A. O. Elzoghby, N. I. Saad, M. W. Helmy, W. M. Samy and N. A. Elgindy, *Eur. J. Pharm. Biopharm.*, 2013, **85**, 444–451.
- 36 A. O. Elzoghby, M. W. Helmy, W. M. Samy and N. A. Elgindy, *Pharm. Res.*, 2013, **30**, 2654–2663.
- 37 N. Elgindy, K. Elkhodairy, A. Molokhia and A. Elzoghby, *J. Nanomed. Nanotechnol.*, 2011, **2**, 110–118.
- 38 N. Bertrand, J. Wu, X. Xu, N. Kamaly and O. C. Farokhzad, *Adv. Drug Deliv. Rev.*, 2014, **66**, 2–25.
- 39 R. K. Jain and T. Stylianopoulos, *Nat. Rev. Clin. Oncol.*, 2010, **7**, 653–664.
- 40 S. K. Hobbs, W. L. Monsky, F. Yuan, W. G. Roberts, L. Griffith, V. P. Torchilin and R. K. Jain, *Proc. Natl. Acad. Sci. U. S. A.*, 1998, **95**, 4607–4612.
- 41 P. N. Sojitra, K. C. Patel and H. S. Patel, *High Perform. Polym.*, 2010, 974–988.
- 42 H. H. A. M. Hassan, A. F. El-Husseiny, A. G. Abo-Elfadl, A. El-Faham and F. Albericio, *J. Macromol. Sci. Part A*, 2012, **49**, 41–54.
- 43 A. El-Faham, H. H. Hassan and S. N. Khattab, *Chem. Cent. J.*, 2012, **6**, 128.
- 44 H. Horowitz and G. Metzger, *Anal. Chem.*, 1963, **35**, 1464–1468.
- 45 H. E. Kissinger, *Anal. Chem.*, 1957, **29**, 1702–1706.
- 46 H. R. Oswald and E. Dubler, *Thermal Analysis*, 1972, vol. 2.
- 47 I. P. Khullar and U. Agarwala, *Can. J. Chem.*, 1975, **53**, 1165–1171.
- 48 M. L. Dhar and O. Singh, *J. Therm. Anal. Calorim.*, 2005, **37**, 259–266.
- 49 G. O. Piloyan, I. D. Ryabchikov and O. S. Novikova, *Nature*, 1966, **212**, 1229–1229.
- 50 K. G. Mallikarjun and R. S. Naidu, *Thermochim. Acta*, 1992, **206**, 273–278.
- 51 J. S. Chawla and M. M. Amiji, *Int. J. Pharm.*, 2002, **249**, 127–138.
- 52 D. B. Shenoy and M. M. Amiji, *Int. J. Pharm.*, 2005, **293**, 261–270.
- 53 S. M. Moghimi and A. C. Hunter, *Trends Biotechnol.*, 2000, **18**, 412–420.
- 54 S. Stolnik, B. Daudali, A. Arien, J. Whetstone, C. R. Heald, M. C. Garnett, S. S. Davis and L. Illum, *Biochim. Biophys. Acta - Biomembr.*, 2001, **1514**, 261–279.
- 55 L. A. G. Rodriguez, L. Cea-Soriano, S. Tacconelli and P. Patrignani, in *Prospects for Chemoprevention of Colorectal Neoplasia*, Springer Berlin Heidelberg, 2013, pp. 67–93.
- 56 T. J. Maier, A. Janssen, R. Schmidt and G. Geisslinger, *FASEB J.*, 2005, **19**, 1353–1355.
- 57 X.-B. Xiong, A. Falamarzian, S. M. Garg and A. Lavasanifar, *J. Control. Release*, 2011, **155**, 248–261.
- 58 A. Kroll, M. H. Pillukat, D. Hahn and J. Schnekenburger, *Arch. Toxicol.*, 2012, **86**, 1123–1136.
- 59 X. R. Song, Z. Cai, Y. Zheng, G. He, F. Y. Cui, D. Q. Gong, S. X. Hou, S. J. Xiong, X. J. Lei and Y. Q. Wei, *Eur. J. Pharm. Sci.*, 2009, **37**, 300–305.
- 60 P. M. Dhabu and K. G. Akamanchi, *Drug Dev. Ind. Pharm.*, 2002, **28**, 815–821.

Graphical abstract



The feasibility of s-triazine polyamides to fabricate celecoxib-loaded nanoparticles.